

WMAP confirming the ellipticity in BOOMERanG and COBE CMB maps

V.G.Gurzadyan^{1,2}, P.A.R.Ade³, P. de Bernardis⁴, C.L.Bianco², J.J.Bock⁵, A.Boscaleri⁶, B. P. Crill⁷, G. De Troia⁴, E.Hivon⁸, V.V.Hristov⁷, A.L.Kashin¹, H.Kuloghlian¹, A.E.Lange⁷, S.Masi⁴, P.D.Mauskopf³, T.Montroy⁹, P. Natoli¹⁰, C.B.Netterfield¹¹, E.Pascale⁶, F.Piacentini⁴, G.Polenta⁴, J.Ruhl⁹, G.Yegorian¹

¹ Yerevan Physics Institute (Armenia)

² ICRA, Dipartimento di Fisica, University La Sapienza, Roma (Italy)

³ Department of Physics and Astronomy, Cardiff (UK)

⁴ Dipartimento di Fisica, University La Sapienza, Roma (Italy)

⁵ JPL, Pasadena (USA)

⁶ IFAC-CNR, Firenze (Italy)

⁷ Caltech, Pasadena (USA)

⁸ IPAC, Pasadena (USA)

⁹ Department of Physics, U.C. Santa Barbara (USA)

¹⁰ Dipartimento di Fisica, Tor Vergata, Roma, (Italy)

¹¹ Department of Physics, University of Toronto (Canada)

Abstract - The recent study of BOOMERanG 150 GHz Cosmic Microwave Background (CMB) radiation maps have detected ellipticity of the temperature anisotropy spots independent on the temperature threshold. The effect has been found for spots up to several degrees in size, where the biases of the ellipticity estimator and of the noise are small. To check the effect, now we have studied, with the same algorithm and in the same sky region, the WMAP maps. We find ellipticity of the same average value also in WMAP maps, despite of the different sensitivity of the two experiments to low multipoles. Large spot elongations had been detected also for the COBE-DMR maps. If this effect is due to geodesic mixing and hence due to non precisely zero curvature of the hyperbolic Universe, it can be linked to the origin of WMAP low multipoles anomaly.

1 Introduction

The CMB experiments of the recent years provided a solid background for understanding the structure and early evolution of the Universe. The comparison of the results of independent experiments has led to satisfactory

mutual agreement. Excellent statistical agreement was found by comparing measurements of the angular power spectrum of the anisotropy detected by different experiments. Moreover, the maps of the BOOMERanG [1], [2], [3], [4], MAXIMA and ARCHEOPS [5] experiments have been recently compared "pixel to pixel" to the high quality maps from the WMAP satellite and excellent agreement was found [6], [7].

In the present article we will study the WMAP map [8] for the region coinciding with the BOOMERanG one, to study the distortion found in 150 GHz Boomerang maps. The latter showed ellipticity for hot and cold anisotropy areas (spots) about 2.2 (2.5 for several degree areas) invariant to the temperature threshold within its certain interval [9]. The effect was detected both for small areas, i.e. containing from several to 10 pixels, but also for larger ones, with over 100 pixels. The latter spots are larger than the scale of the horizon at the last scattering surface. The biases of the estimator and of the noise are negligible for the larger areas [10]. If this ellipticity effect, first detected for the COBE-DMR data [11], is due to the geodesic mixing [12], then it might indicate a non precisely zero curvature of the Universe, and hence be related with the origin of the low CMB multipoles anomaly detected by WMAP (see e.g. [13, 14, 15, 16]). The study below of the ellipticity in the WMAP maps, on the same region observed by BOOMERanG, acts also as an additional comparison of the results of the two experiments.

Measuring the ellipticity in the CMB maps actually implies the estimation of the Kolmogorov-Sinai (KS) entropy of the dynamical process which might lead to that effect (the geodesic mixing or whatever). This is based on the essential fact that, KS-entropy being local (in time) characteristics of the dynamical system, enable to determine the properties of the evolution of the system. With the CMB we have an analogous problem: having the maps, i.e. the parameters of the moving photon beams of various temperature at present epoch, we aim to recover their former history.

2 CMB maps and geodesic mixing

The property of mixing of geodesic flows in hyperbolic spaces applied to the freely moving CMB photons can lead to ellipticity in the maps [12]. In a hyperbolic space of maximally symmetric metric the geodesic flow f^t is an Anosov system [17] with the following remarkable properties. The tangential space $TM_{f^t(x)}$ can be split into exponentially converging and deviating subspaces $E^s(f^t(x)), E^u(f^t(x))$ (at $t \rightarrow \infty$ and $t \rightarrow -\infty$) of the

tangential space, so that

$$\begin{aligned} TM_{f^t(x)} &= E^s(f^t(x)) \oplus E^u(f^t(x)), \\ df^\tau E^s(f^t(x)) &= E^s(f^{t+\tau}(x)), \quad df^\tau E^u(f^t(x)) = E^u(f^{t+\tau}(x)), \end{aligned}$$

and for all $t > 0$, one has

$$\begin{aligned} \| df^t v \| &\leq C e^{-\lambda t} \| v \|, & v \in E^s(f^t(x)); \\ \| df^t v \| &\geq C^{-1} e^{\lambda t} \| v \|, & v \in E^u(f^t(x)), \end{aligned}$$

where $C > 0, \lambda > 0$. The following from here the exponential decay of the time correlation function of the geodesic flow

$$|b(t)| \leq |b(0)| e^{-c\chi t}, c > 0. \quad (1)$$

determines the strong chaotic (mixing) properties of the bundle [18]. Photon beams of various temperature mix by exponential rate which will lead to the isotropization of the CMB and to distortion of the maps. For Friedmann-Robertson-Walker Universe the parameter χ is the KS-entropy and is determined by a single scale, the diameter of the Universe, $\chi = 1/a$ [12]. A different origin of the elongation in CMB maps is certainly not excluded, and for more accurate maps the Kolmogorov complexity of the anisotropy areas can be the most informative descriptor for distinguishing the effect [19].

3 Maps

The region observed by BOOMERanG is at high Galactic latitudes, and covers about 4% of the southern sky, with coordinates $RA > 70^\circ$, $-55^\circ < dec < -35^\circ$ and $b < -20^\circ$. The map analyzed here contains 33111 pixels, each of 7 arcmin [1],[2], [20], [21], [22]. BOOMERanG's obtained high resolution ($\sim 10'$) maps of the microwave sky in 4 different channels, at 90, 150, 240 and 410 GHz.

Two maps from two independent detectors at 150 GHz have been used for the ellipticity study [9]. Those maps have been obtained from the time ordered data using an iterative procedure [23], which properly takes into account the system noise and produces a maximum likelihood map. The structures of scales larger than 10° were removed in this procedure, to avoid the effects of instrument drifts and of 1/f noise. Three known AGN's have been excluded from the analysis of the region.

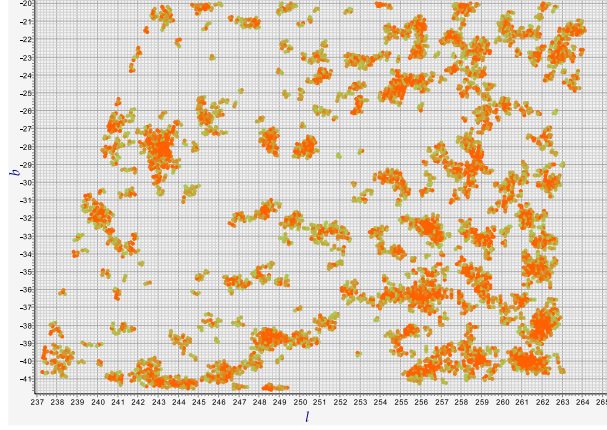


Figure 1: Pixels higher than $100 \mu K$ in the BOOMERanG "sum" or "A+B" map obtained from three independent measurement channels at 150 GHz: $A+B = B150A + (B150A1 + B150A2)/2$. The pixel size is 6.9 arcmin (Healpix npix=512). The measurement units (μK) refer to thermodynamic temperature fluctuations of 2.73K blackbody.

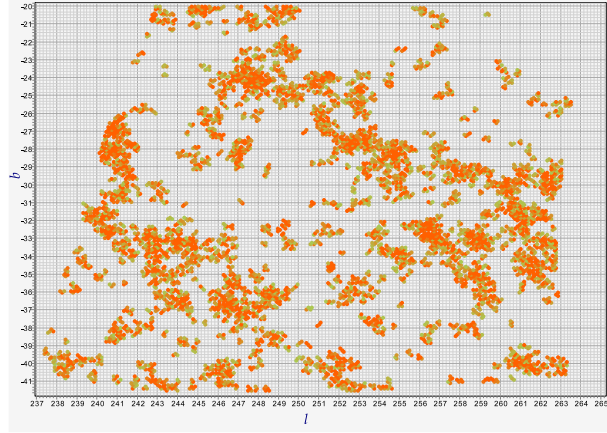


Figure 2: The WMAP sum map of V and W channels for the same thresholds as in Fig.1, and in the same sky region.

The WMAP first-year maps have been obtained from the publicly available, monopole and dipole-removed datasets for channels W and V (frequencies 61 and 94 GHz, respectively). The noise per $28'$ pixel in those maps is about $35 \mu K$, to be compared to a noise of $\sim 25 \mu K$ per $28'$ pixel in the 150GHz map of BOOMERanG. For comparison of the two datasets we chose two sky regions. The first one coincides with the BOOMERanG region; the second one has galactic coordinates $l=181^\circ.33 - 209^\circ.23$ and $b= -20^\circ.03 - -41^\circ 60$. The two regions have very similar size.

Figures 1-3 show the BOOMERANG and the two WMAP maps, respectively, at temperature thresholds higher than $100 \mu K$.

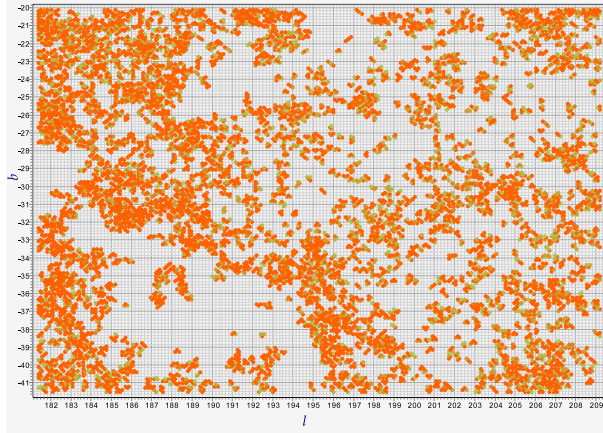


Figure 3: The WMAP sum map for the same thresholds as in Fig.1, in a sky region different from the BOOMERanG one, but with similar size. The structure is visually different from the one of Fig.2, due to the value of the lowest multipoles in the two regions. This fact, however, does not affect the ellipticity results.

4 Analysis

We have used the same algorithms in the definition of the excursion sets (areas), their centers and the ellipticities, which were used for the BOOMERanG maps [9]. The study of the same sky region will obviously reveal the differences of the parameters of the datasets and hence their role in the studied effect. Areas, as usual, are defined as pixel sets with temperature equal and higher than a given temperature threshold and lower, for negative thresh-

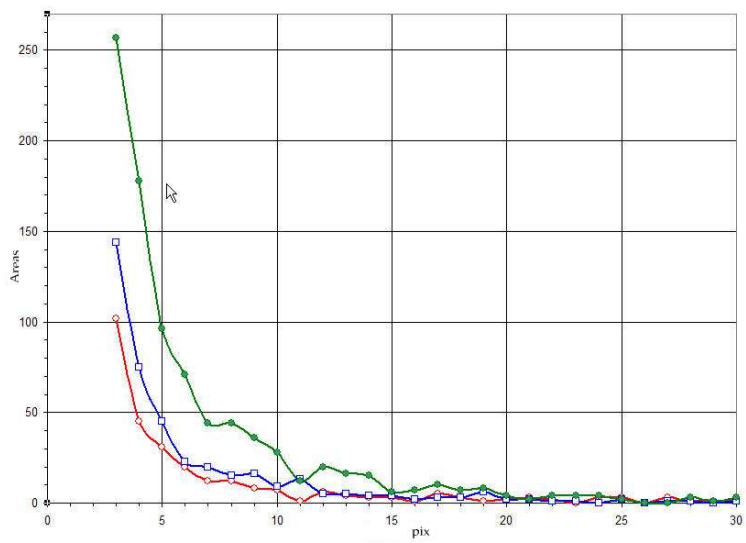


Figure 4: Number of the anisotropy areas vs the size of each area (in number of pixels) in the maps of Figs.1-3. : BOOMERanG (empty circles), WMAP in the same region (squares), WMAP in another region (filled circles).

olds. Fig.4 shows the number of areas vs the size of areas (in pixels) for the 3 maps. We defined the center as of the middle point of the coordinates of extremal pixels of the area: we have checked that this coincides with the center of inertia of the areas with an accuracy of few arc minutes.

The bias of the ellipticity estimator due to the noise was up to 0.4 and up to 0.3 for BOOMERanG maps. However for larger areas (more than 100 pixels), such bias is much smaller, less than 0.1 [9]. These values are applicable to the WMAP data as well, since, as mentioned above, the noise level is comparable to the one of BOOMERanG.

The results of the computations are shown in Fig. 5. The existence of threshold independent ellipticity is evident, with an average value similar to the one in the BOOMERanG maps, both for small and large areas. The effect exists also when channel V is changed to channel W. The obliquities of the areas did not show any preferred direction, as it was for BOOMERanG.

Obviously the small pixel areas are clearly defined at higher temperature thresholds and loose their identity towards lower thresholds (forming complex connected regions). Larger areas (e.g. more than 100-pixel) on the other hand, are not too many at higher thresholds and hence their 'exis-

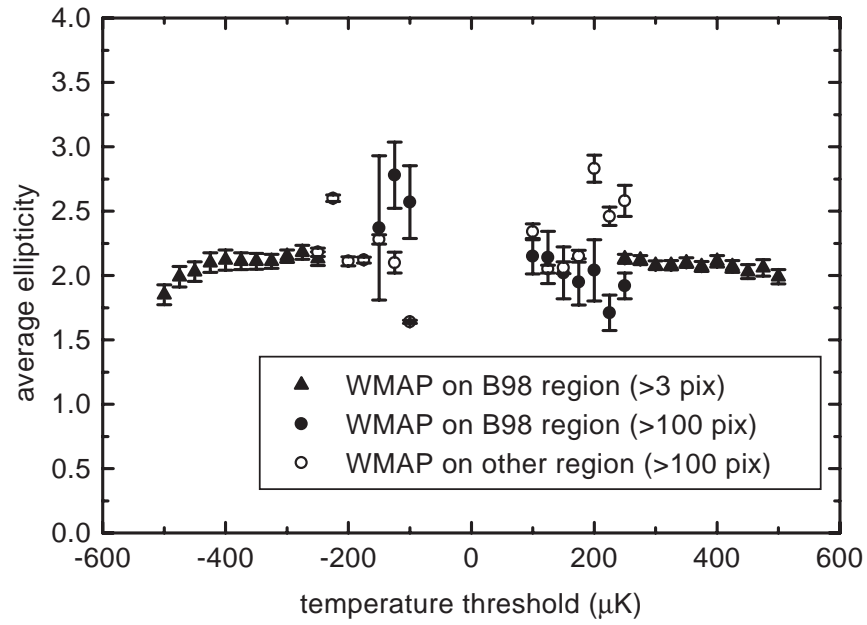


Figure 5: Ellipticity vs temperature threshold for the anisotropy areas containing more than 3 pixels (triangles), more than 100 pixels (filled circles) in WMAP map of Fig.2, and for anisotropy areas with more than 100 pixels in the WMAP map of Fig.3 (circles).

tence' threshold interval is relatively smaller. This explains the intervals of the points on Fig.5 (for more details see [9]).

While the WMAP's map in Fig.3 clearly differs from the BOOMERanG field (Figs.1,2) due to the low multipoles, the ellipticity of the large spots is again around 2.5, as found for BOOMERanG, with an unavoidable scatter due to small-numbers statistics. For areas with up to 100-pixel the WMAP data are impressive, both because of their stability versus threshold and because of their value, fully confirming the results of the ellipticity analysis of the BOOMERanG map.

5 Conclusions

The analysis of WMAP maps in the same region observed by BOOMERanG detects ellipticity of anisotropies of the same average value (around 2), as found for BOOMERanG, even though there is difference in the maps at least due to the absence of low multipoles in the BOOMERanG data. Ellipticity for large scale areas had been found also in COBE-DMR maps [11]. The WMAP data confirm the effect for scales both smaller and larger than the horizon at the last scattering surface. This suggests that the effect is not due to physical effects at the last scattering surface, and can arise after, while the photons are moving freely in the Universe. As a large-scale effect this can be related to the WMAP low multipole anomaly, since the geodesics mixing and the low multipoles are both related to the diameter of the Universe - the first one via hyperbolic geometry, the second one, via boundary conditions - and possibly even with vacuum's relevant modes' contribution to the dark energy [24].

References

- [1] de Bernardis P., et al, 2000, Nature, 404, 955.
- [2] de Bernardis P., et al, 2002, ApJ, 564, 559.
- [3] Netterfield C.B., et al, 2002, ApJ, 571, 604.
- [4] Ruhl J., et al, 2003, ApJ, 599, 786.
- [5] Benoit A., et al., 2003, A&A, 399, L19.
- [6] de Bernardis P., et al, astro-ph/0311396

- [7] Abroe M.E., et al., 2003, astro-ph/0308355
- [8] Bennett C.L., et al., 2003, ApJ Suppl. 148, 1.
- [9] Gurzadyan V.G., Ade P.A.R., de Bernardis P. et al, 2003, Int.J.Mod.Phys. D, 12, 1859.
- [10] Gurzadyan V.G., Ade P.A.R., de Bernardis P. et al, astro-ph/0312305
- [11] Gurzadyan V.G., Torres S., 1997, A & A, 321, 19.
- [12] Gurzadyan V.G., Kocharyan A.A., 1992, A&A, 260, 14; Europhys. Lett. 1993, 22, 231.
- [13] Aurich R., Steiner F., 2003, astro-ph/0302264
- [14] Efstathiou G., 2003, MNRAS, 343, L95.
- [15] Uzan J-P., Kirchner U., Ellis G.F.R., 2003, MNRAS, 344, L65.
- [16] Luminet J.-P. et al, 2003, Nature, 425, 593.
- [17] Anosov D.V. , 1967, Comm. Steklov Mathematical Inst., vol.90.
- [18] Lockhart C.M., Misra B., Prigogine I. 1982, Phys.Rev. D25, 921.
- [19] Gurzadyan V.G., 1999, Europhys.Lett., 46, 114.
- [20] Piacentini F. et al, 2002, Ap.J.Suppl., 138, 315.
- [21] Masi et al 2001, ApJ 553, L93.
- [22] Crill B.P. et al, 2002, astro-ph/0206254
- [23] Natoli P., et al., 2001, A&A 371, 346.
- [24] Gurzadyan V.G., Xue S.S. 2003, Mod.Phys.Lett. 18, 561.